Nuclear Instruments and Methods in Physics Research 228 (1985) 377–386
North-Holland, Amsterdam

DERIVATIVE UNFOLDING BY SPLINE TECHNIQUES

K.V. SUBBAIAH and A. NATARAJAN

Safety Research Laboratory, Reactor Research Centre, Kapakkam, Tamilnadu, 603102, India

Received 19 July 1984

This paper presents some possible improvements to the derivative unfolding scheme employed in processing recoil proton data to obtain the neutron spectra. The scheme is based on representing the recoil proton spectrum by means of equally spaced cubic bell-splines. The finite spread in the detector response to monoenergetic protons is accounted for by folding the splines suitably. A code based on this formulation has been tested with trial spectra pertaining to standard neutron sources such as Pu–Be and has performed better in terms of resolution and of accuracy of the predicted peak positions. The current formulation is flexible for adding constraints using a priori information. This is demonstrated with respect to the suppression of spurious oscillations occurring near the high energy end of the spectra. This scheme is restricted to continuous spectra, however.

1. Introduction

The need for unfolding the experimental count spectra to obtain the true radiation spectra is well recognised. The computational formulation needed for this purpose almost always leads to a system of ill-conditioned equations, whose solutions are highly sensitive to the inherent statistical noise present in the data as well as to the finite precision used in the computations. The numerical instability aspect of the problem has been dealt with by various means, notable among them being the regularization procedure developed by Tikhanov [1]. With specific reference to neutron spectrometry using recoil proton measurements, several codes are available, the best known among them being FERDOR [2]. It makes use of the regularization method to enforce the non-negativity constraint on the solution. While FERDOR is of general applicability, it calls for significant efforts in terms of generating the detector response functions and involves a fair amount of computer time as well. Also, its accuracy is strongly dependent on the generated response functions.

In the case of small detectors for which the response can be assumed to be due to essentially single collisions with isotropic distribution in the center of mass coordinate system, simpler procedures based on the derivative unfolding are possible and are in wide use. By virtue of the idealized response, an exact inversion of the folding equation is possible and calls for only the derivative of the recoil proton spectrum. In the above sense, the numerical instabilities normally associated with the unfolding process are largely absent in this method. Difficulties arise, however, from having to obtain the derivatives from discrete data. Generally, these are solved by taking recourse to some form of smoothing. DUFOLD, PSNS-N and MATXUF [3–5] codes for neutron spectral unfolding can be cited as examples in this instance. The first two codes employ least-squares criterion for obtaining a smoothed representation of the pulse-height data using piece-wise polynomials. The requisite derivatives then follow analytically. Johnson [6] has reported that the least-squares smoothing procedure as employed in these codes is susceptible to errors and can cause spectral hardening. Further, when a variable number of points are used in smoothing the data, the area under the peak is not conserved, and in extreme cases even spurious peaks appear. MATXUF code employs an alternative approach suggested by him, wherein the smoothing is applied not to the pulse-height data but to the resulting spectrum after unfolding. The smoothing by Gaussian window function is similar to the one found in FERDOR.

This paper presents a derivative unfolding scheme, based on cubic bell-splines, which is free from the earlier cited errors but still has the advantages of the least-squares procedure such as the possibility of

adding constraints based on a priori information. The choice of splines is due to the fact that they lead to a more accurate determination of the derivatives from discrete data. Besides, the built-in continuity conditions of splines enable a global least squares approach, ensuring a uniform degree of smoothing. The scheme employed here leads to enhanced resolution as well as to an improved estimate of the peak positions.

2. Formulation

Under the idealized response conditions mentioned earlier, the spectrum $N(E)$ of a flux of neutrons incident on a detector and the corresponding recoil proton spectrum $P(E)$ are related by the simple expression

$$N(E) = -(E/\varepsilon)(\mathrm{d}P/\mathrm{d}E), \tag{1}$$

where ε corresponds to the detection efficiency for neutrons of energy E. The recoil proton distribution is not directly measurable and is conventionally replaced by the measured pulse-height distribution. Such a procedure ignores the finite spread in the detector response to protons, leading to an overall loss in the resolution, and also possibly to an erroneous prediction of the peak positions. However, this deficiency can be set right by an initial unscrambling of the pulse-height data to obtain the required recoil proton distribution. For this purpose, the pulse-height distribution $C(E)$ is written as

$$C(E) = \frac{1}{\sqrt{2\pi}} \int_0^\infty P(E') \exp\left\{ \frac{-[(E'-E)/\sigma(E')]^2}{2} \right\} \frac{\mathrm{d}E'}{\sigma(E')}. \tag{2}$$

In writing eq. (2), the detector response to monoenergetic protons of energy E has been assumed to be Gaussian with spread $\sigma(E)$. Towards a numerically stable solution of this equation, it is necessary to enforce some auxilliary conditions on $P(E)$. Since the derivative approach to unfolding is best suited to applications involving the continuous neutron spectra, demanding the continuity and smoothness of $P(E)$ could itself serve as conditions. Accordingly, $P(E)$ is approximated by piece-wise polynomials which are represented here by splines as follows:

$$P(E) = \sum_{j=1}^{n} a_j S_j(E), \tag{3}$$

where $S_j(E)$ corresponds to a cubic bell-spline centered at the energy knot E_j, the coefficient a_j corresponds to its strength, and n represents the total number of splines. The bell-splines $S_j(E)$ are defined as follows [7]:

$$\begin{aligned}
S_j(E) &= \left\{(E - E_{j-2})/(E_{j-1} - E_{j-2})\right\}^3, && E_{j-2} \leqslant E \leqslant E_{j-1};\\
&= 1 + 3\left\{\frac{E - E_{j-1}}{E_j - E_{j-1}}\right\} + 3\left\{\frac{E - E_{j-1}}{E_j - E_{j-1}}\right\}^2 - 3\left\{\frac{E - E_{j-1}}{E_j - E_{j-1}}\right\}^3, && E_{j-1} \leqslant E \leqslant E_j;\\
&= 1 + 3\left\{\frac{E_{j+1} - E}{E_{j+1} - E_j}\right\} + 3\left\{\frac{E_{j+1} - E}{E_{j+1} - E_j}\right\}^2 - 3\left\{\frac{E_{j+1} - E}{E_{j+1} - E_j}\right\}^3, && E_j \leqslant E \leqslant E_{j+1};\\
&= \left\{(E_{j+2} - E)/(E_{j+2} - E_{j+1})\right\}^3, && E_{j+1} \leqslant E \leqslant E_{j+2};\\
&= 0, && \text{otherwise.}
\end{aligned} \tag{4}$$

The above definition ensures that $S_j(E)$ and its first two derivatives are continuous everywhere. Only equally spaced splines are considered here, and the optimum spacing between adjacent spline knots is

discussed later. Using expression (3), eq. (2) can be rewritten as

$$C(E) = \sum_{j=1}^{n} a_j G_j(E), \tag{5}$$

where

$$G_j(E) = \frac{1}{\sqrt{2\pi}} \int_0^{\infty} S_j(E') \exp\left\{ - \frac{[(E'-E)/\sigma(E')]^2}{2} \right\} \frac{\mathrm{d}E'}{\sigma(E')}.$$

The folded splines $G_j(E)$ are evaluated numerically. The unknown coefficients a_j are estimated by minimizing the functional

$$F(a_1, a_2, \ldots, a_n) = \int_0^{\infty} \{C(E) - a_j G_j(E)\}^2 W(E)\, \mathrm{d}E, \tag{6}$$

where $W(E)$ corresponds to a weight function and is inversely proportional to the variance in observed counts. Since $C(E)$, the count rate, is available only as discrete data, eq. (6) takes the form

$$\begin{aligned} F(a_1, a_2, \ldots, a_n) &= \sum_{i=1}^{m} \left\{ C(E_i) - \sum_{j=1}^{n} a_j G_j(E_i) \right\}^2 W_i, \\ &= \sum_{i=1}^{m} \left\{ c_i - \sum_{j=1}^{n} a_j G_{ij} \right\}^2 W_i, \quad m > n, \end{aligned} \tag{7}$$

where the quadrature weights have been absorbed into W_i. In matrix notation eq. (7) can be written as

$$F(\boldsymbol{A}) = (\boldsymbol{C} - \mathbf{G}\boldsymbol{A})^{\mathrm{T}} \mathbf{W} (\boldsymbol{C} - \mathbf{G}\boldsymbol{A}), \tag{8}$$

where

$$\boldsymbol{C}^{\mathrm{T}} = (c_1, c_2, \ldots, c_m), \quad \boldsymbol{A}^{\mathrm{T}} = (a_1, a_2, \ldots, a_n).$$

It can be readily shown that the minimization of $F(\boldsymbol{A})$ leads to

$$\boldsymbol{A} = (\mathbf{G}^{\mathrm{T}}\mathbf{W}\mathbf{G})^{-1}\mathbf{G}^{\mathrm{T}}\mathbf{W}\boldsymbol{C}. \tag{9}$$

Using the a_j coefficients obtained from eq. (9), and combining eqs. (1) and (3) the neutron flux spectrum can be written as,

$$N(E) = \boldsymbol{U}^{\mathrm{T}}\boldsymbol{A},$$

where

$$u_j(E) = -(E/\epsilon)\left(\mathrm{d}S_j(E)/\mathrm{d}E\right). \tag{10}$$

However, the neutron spectra obtained in this way are subject to undue oscillations at the high energy end. This is to be expected, since the incident neutron flux in this region is usually small. Coupled with low efficiency, this leads to poor statistics and consequent numerical instabilities. Therefore, the high energy end of spectrum calls for some additional treatment. The fact that both the neutron and recoil proton spectra vanish beyond some maximum energy, say $E_{\max}$, can be utilized for this purpose. Accordingly, expression (7) is minimized subject to the conditions that

$$P(E_{\max}) = 0, \quad P'(E_{\max}) = 0. \tag{11}$$

By choosing the $(n-1)$th spline knot to correspond to E_{max}, these conditions can be translated as

$$a_{n-2} + 4a_{n-1} + a_n = 0, \quad 3a_{n-2} - 3a_n = 0.$$

Or equivalently

$$\boldsymbol{Q}^{\mathrm{T}}\boldsymbol{A} = 0, \quad \boldsymbol{R}^{\mathrm{T}}\boldsymbol{A} = 0.$$

where

$$\boldsymbol{Q}^{\mathrm{T}} = (0, 0, 0, \ldots, 1, 4, 1), \quad \boldsymbol{R}^{\mathrm{T}} = (0, 0, 0, \ldots, 3, 0, -3).$$

It is well known that minimizing $F(\boldsymbol{A})$ with the constraints given by eq. (11) is equivalent to minimizing the modified functional:

$$F(\boldsymbol{A}) = (\boldsymbol{C} - \mathbf{G}\boldsymbol{A})^{\mathrm{T}}\mathbf{W}(\boldsymbol{C} - \mathbf{G}\boldsymbol{A}) + \alpha \boldsymbol{A}^{\mathrm{T}}\boldsymbol{Q}\boldsymbol{Q}^{\mathrm{T}}\boldsymbol{A} + \beta \boldsymbol{A}^{\mathrm{T}}\boldsymbol{R}\boldsymbol{R}^{\mathrm{T}}\boldsymbol{A}, \tag{12}$$

where α and β are the Lagrange multipliers, and their values provide a measure of the degree to which the constraints are enforced. The solution in this case can be written as

$$\boldsymbol{A} = \left[\mathbf{G}^{\mathrm{T}}\mathbf{W}\mathbf{G} + \alpha \boldsymbol{Q}\boldsymbol{Q}^{\mathrm{T}} + \beta \boldsymbol{R}\boldsymbol{R}^{\mathrm{T}}\right]^{-1}\mathbf{G}^{\mathrm{T}}\mathbf{W}\boldsymbol{C}, \tag{13}$$

where α and β are left to be decided by a parametric study.

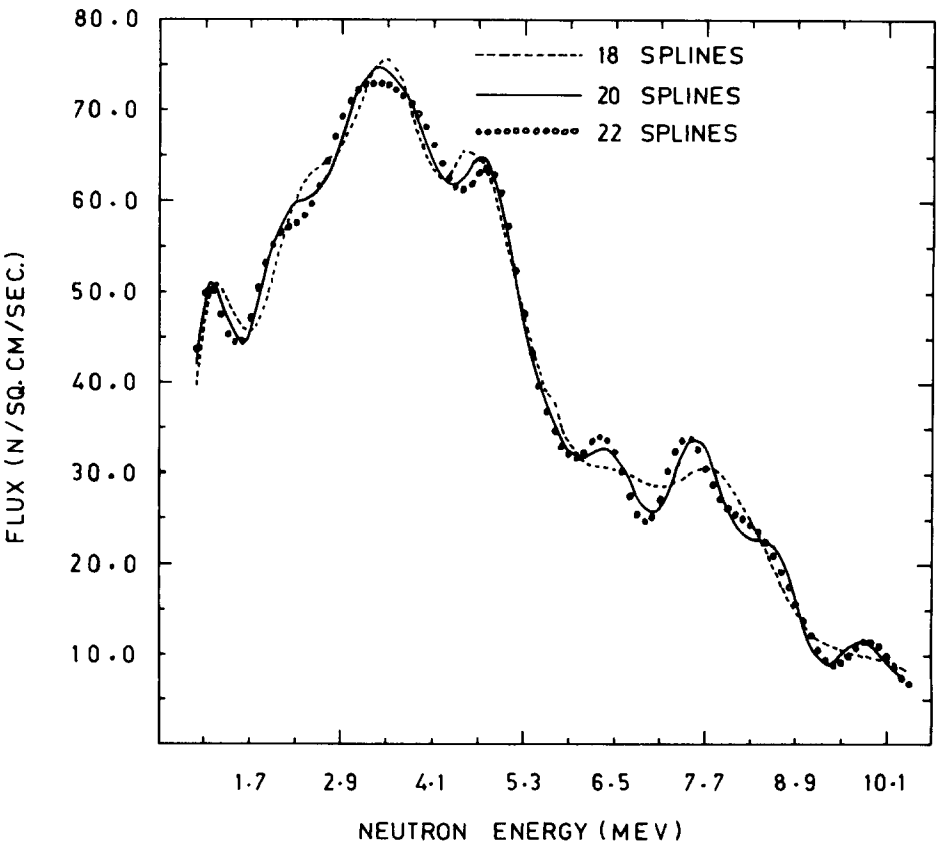

Fig. 1. Unfolded Pu–Be spectra with different numbers of cubic splines.

For $m \gg n$, (which is usually the case) an interval estimate for this problem is approximately given by

$$N = \boldsymbol{U}^{\mathrm{T}}\boldsymbol{A} \pm k\sqrt{\boldsymbol{U}^{\mathrm{T}}H^{-1}\mathbf{G}^{\mathrm{T}}\mathbf{W}\mathbf{G}H^{-1}\boldsymbol{U}}, \tag{14}$$

where

$$H = \mathbf{G}^{\mathrm{T}}\mathbf{W}\mathbf{G} + \alpha QQ^{\mathrm{T}} + \beta RR^{\mathrm{T}}.$$

The constant k depends on the degree of confidence desired and is determined from a χ^2-distribution whose degrees of freedom equal the number of splines used.

3. Code development and evaluation

Based on the above formulation a computer code – DUST (derivative unfolding by spline techniques) – has been written in FORTRAN IV, which can be operated on the microcomputer PDP 11/23. Besides the count spectra, the following data characterizing the detector are required as input:

1) scintillation pulse-height as a function of proton energy,
2) detector efficiency as a function of neutron energy,
3) full width at half-maximum (fwhm) of the pulse-height distribution due to monoenergetic protons as a function of energy.

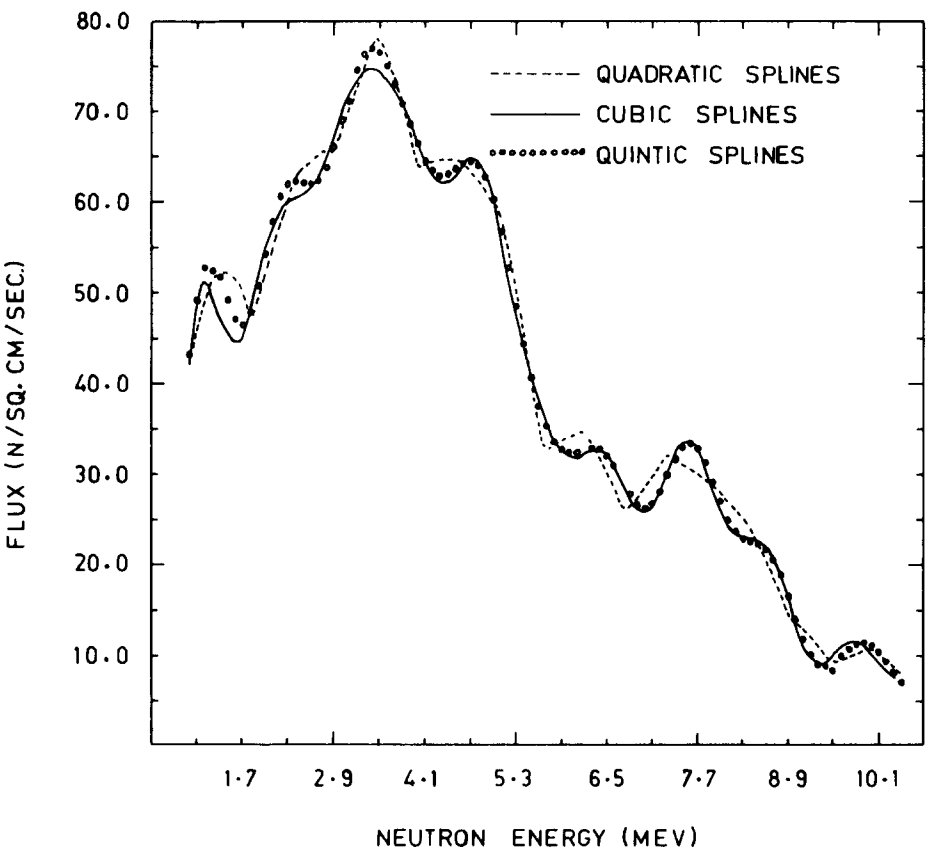

Fig. 2. Unfolded Pu–Be spectra obtained with quadratic cubic and quintic splines.

If needed, the code bins the input counts into approximately equal energy intervals. Both point and interval estimates of the neutron flux are generated as output.

To evaluate the performance of the code, specimen input count spectra pertaining to standard neutron sources such as Pu–Be (α, n) have been unfolded and analysed. Typical results from some of these calculations are presented below.

The selection of an appropriate spacing between spline knots plays a major role in deciding the accuracy and the reliability of the unfolded spectra. In general, a large spline knot spacing would lead to an increased precision of the estimated spline coefficients and incidentally would also reduce the computational effort involved. However, these gains are offset by a corresponding loss in the resolution. An optimum balance between the two is, therefore, necessary. A quantitative investigation of this aspect has been carried out using a sample input data pertaining to Pu–Be spectra obtained from ref. [5]. A number of splines varying from 15 to 25 have been employed to cover the energy range between 0.8 and 10.5 MeV. A choice in the range of 20–22 splines has yielded results that match best with the known Pu–Be spectra [9]. Fig. 1 shows the unfolded spectra obtained with 18, 20 and 22 splines. In the case of 18 splines, the spectrum obtained is reasonably good, although the peaks at around 6.5 and 7.8 MeV are poorly resolved, and the expected peak around 9.5 MeV is barely seen as a hump. When 20 splines are employed to cover the same range, all the peaks become fully resolved and the peak positions shift downwards fitting the known results better. By adding two more splines, only marginal changes in spectra are observed. However,

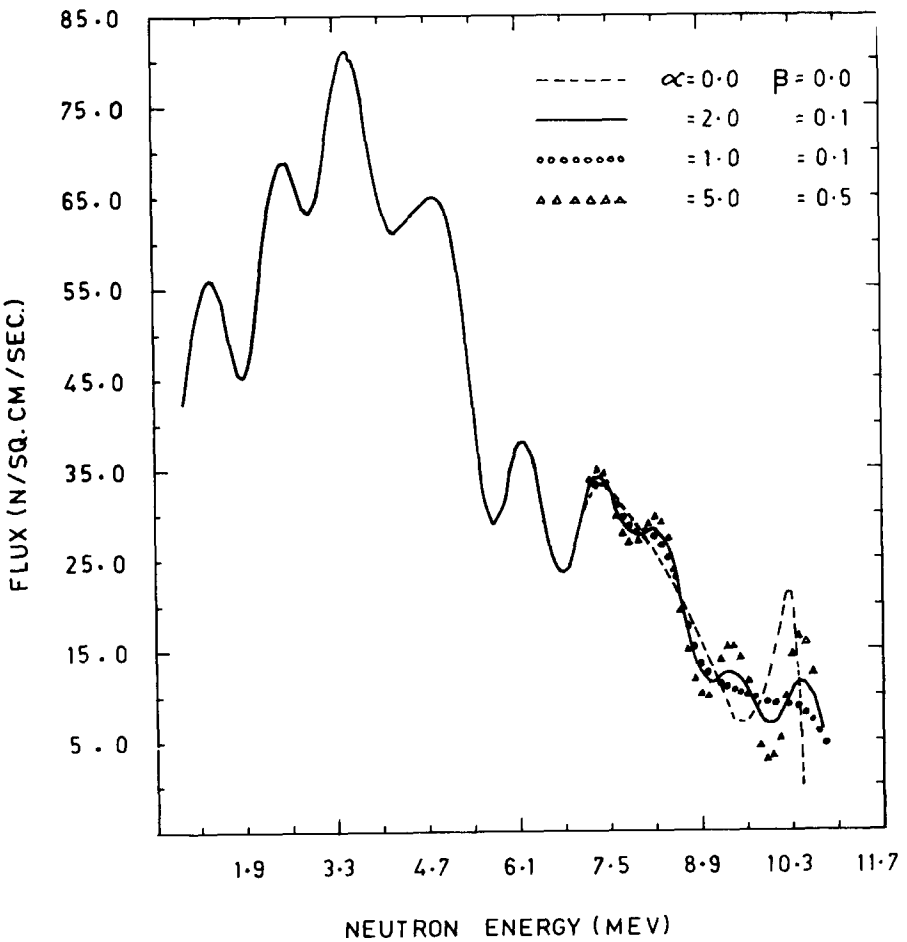

Fig. 3. Comparison of Pu–Be spectra with and without the end-point constraints.

employing too many splines tend to produce large swing (not shown in the figure) in the amplitude of the peaks which in turn leads to negative regions in valleys of low intensity.

A hard and fast rule for selecting the spline knot spacing applicable to all situations is not feasible. However, the following points should provide some guidelines. A cubic spline approximation for the proton spectrum and hence a parabolic approximation of its derivative would imply that there can be utmost one peak or a valley in an interval and that no two adjacent intervals could each contain a peak/valley. This sets the limit of resolution to a minimum of one spline spacing. Hence, the selected spacing between knots should not exceed the minimum anticipated spacing between peaks. Further, the reliability of the estimated parameter warrants that there be at least several count channels falling in each interval. In fact, this is a serious limitation at the low energy end of the spectrum, where the pulse-height response to protons is highly non-linear with respect to energy and a few channels tend to cover fairly large spread in energy.

One may be interested in finding out whether higher order splines would improve the resolution limit of one knot spacing set by the cubic splines. Accordingly, calculations have been made with fourth and fifth order splines, using the same knot spacing as employed in the cubic case. The computational effort involved in these is only marginally higher. Fig. 2 compares the spectra computed with fifth order and cubic splines. These two spectra hardly differ at all. The remarkable agreement of the predicted peak positions lends further credence to the selected spline knot spacing. Just for the sake of completeness, calculations using quadratic splines have also been done and are indicated in the same figure. The

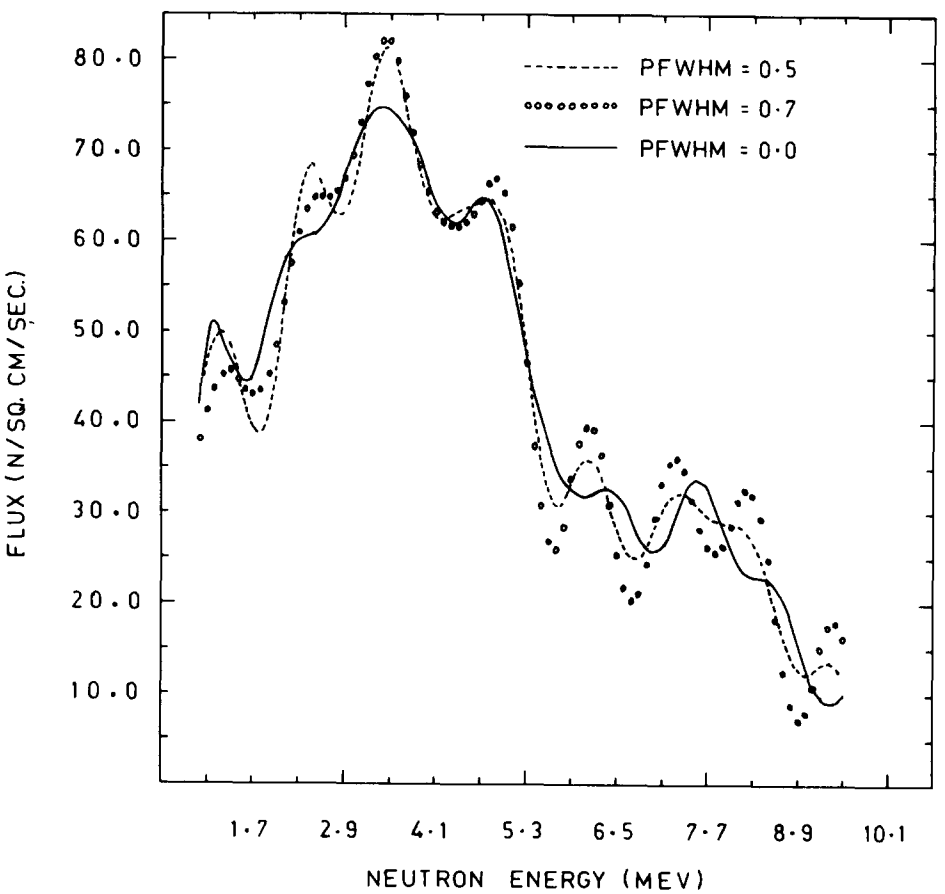

Fig. 4. Pu–Be spectra with and without the inclusion of the finite detector resolution.

significant drop in the resolution of the high energy peaks at 6.5, 7.8 and 9.6 MeV may be noted in this case.

Another feature of the formulation that merits discussion is the weightage given to the end-point (E_{max}) constraints. Fig. 3 shows the spectra of Pu–Be for various values of α and β ranging from 0 to 5 and 0 to 0.5 respectively. In the absence of these constraints, the spectrum around 10.0 MeV shows a large spurious oscillation resulting in negative values beyond 10.4 Mev. A more unpleasant consequence of this oscillation is the distortion of the spectrum close to and below 10.0 MeV. In fact, the expected peak around 9.6 MeV is not seen at all. On including the constraints by changing the values of α and β from zero, the spurious oscillation is observed to come down initially and the peak around 9.6 MeV is restored. But any subsequent increase tends to reintroduce the oscillations. Thus, values of 2.0 for α and 0.1 for β which allow for a minimum level of distortion and negativity can be considered as appropriate for this spectrum. It may be noted that in all these cases the effects of constraints on the spectra are limited to just two or three spline intervals near E_{max}.

The above values of α and β have been used with several different spectra and have been found to be satisfactory [10]. In the context of applying these constraints, it may be observed that the end point energy E_{max} is to to be specified as one of the inputs and is known only approximately. Consistency of this data with experimental data is necessary. In cases where the finite resolution of the scintillation process is ignored, E_{max} can be taken as the energy corresponding to the highest channel with non-zero counts.

It is interesting at this point to see how the spectral shapes are affected by virtue of having taken into

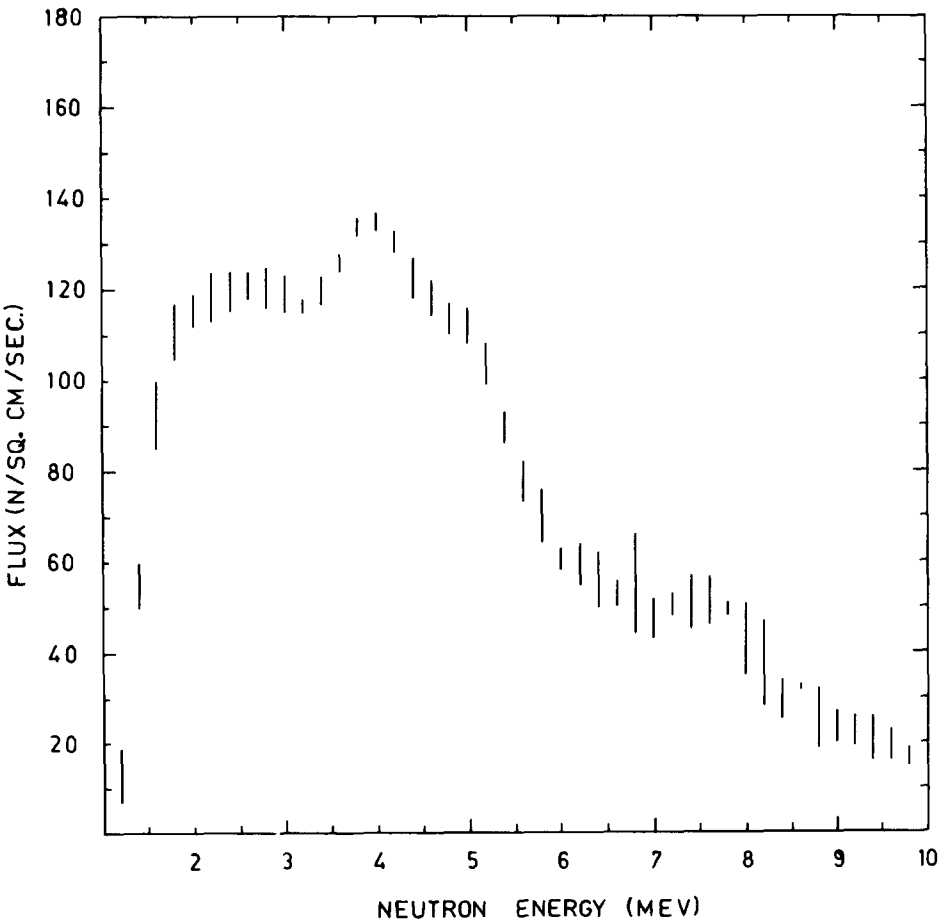

Fig. 5. Dispersion in the point estimates of an Am–Be spectrum over more than 100 trials.

account explicitly the smearing process in scintillation. To enable such a study, the values of fwhm have been multiplied by a scaling factor (PFWHM) varying from 0 to 1. Unfolded spectra of Pu–Be for PFWHM values of 0.0, 0.5 and 0.7 are shown in fig. 4. Obviously, the spectrum with the PFWHM value of 0.0 corresponds to the conventional derivative unfolded one. For PFWHM values of 0.5 and 0.7, the peaks and valleys are significantly accentuated. Also, the positions of the peaks at 6.5, 7.8 and 9.8 MeV shift progressively downwards with increasing PFWHM values. Likewise, the peaks at the low energy end such as at 1.6 and 2.2 MeV have shifted upwards. The intensity of the peak at 1.6 MeV is reduced, though marginally. The shape of the spectrum with the PFWHM values in the range of 0.5 to 0.7 agree well with the known results [9]. Here it may be noted that a correction factor of 0.7 has been indicated by Miller [5] for his fwhm data.

The dispersion in the predicted point estimates of Am–Be spectra over repeated measurements (> 100) is shown in fig. 5. The observed spread in intensity is quite narrow and is generally less than 5% at all energies. The predicted peak positions in these trials have shown a spread of about ± 0.2 MeV, which appears to be quite reasonable. Fig. 6 compares the unfolded spectrum of Pu–Be obtained by the present code with that obtained by MATXUF [5]. For the purpose of the present comparison PFWHM has been set to zero. The agreement between the two spectra is quite good above 5 MeV. Below this energy, while they broadly agree, the spectrum obtained from MATXUF contains several undulations which increase gradually with decreasing energy. The spectrum resulting from the present formulation is, however, smooth and is in accordance with expected results [9].

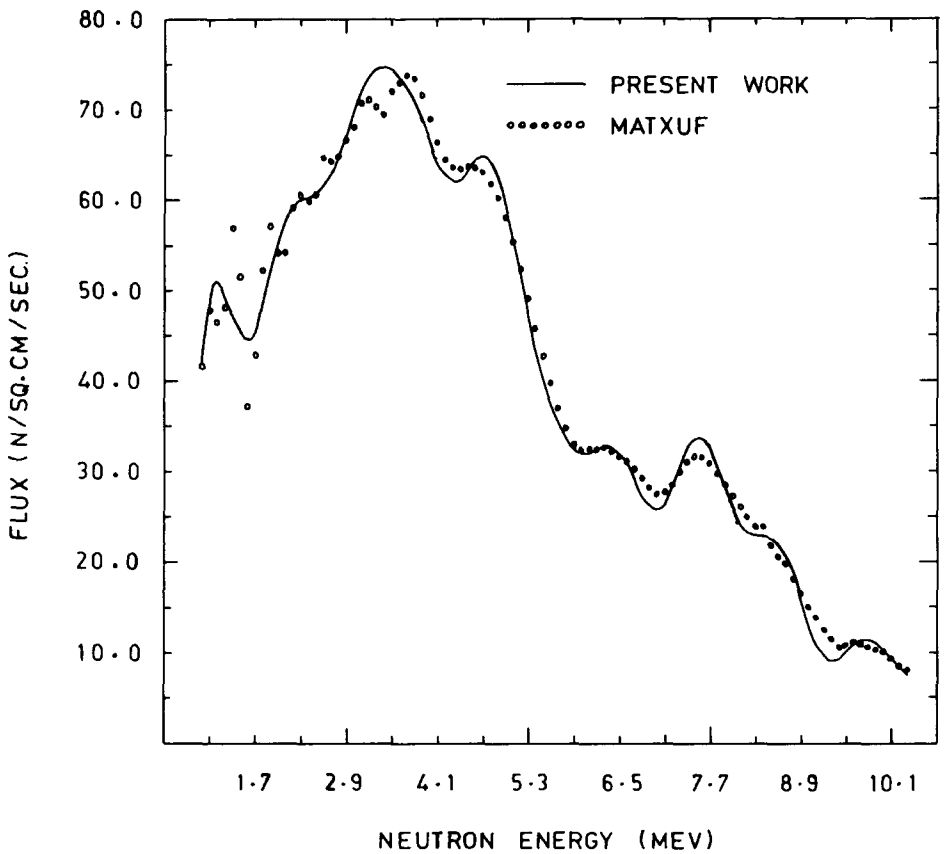

Fig. 6. Comparison of Pu–Be spectra unfolded by different codes.

4. Conclusion

In summary, it is observed that the accounting of the finite resolution of the scintillation process along with the imposition of continuity conditions would lead to enhanced resolution and more accurate peak positions vis-à-vis the past methods of derivative unfolding. The additional computational effort involved in doing so is insignificant. Besides, the present formulation is more flexible for adding any constraints based on a priori information. It is tailor-made, however, to situations involving the continuous neutron spectra.

The authors wish to thank their colleagues V.M. Raghunath and V.M. Sundaram for supplying the more than 100 data sets of Am–Be count spectra used in evaluating the code, and D.V. Gopinath for fruitful discussions. This work was supported in part by an IAEA Research Contract 2253/R1/RB.

References

[1] A.N. Tikhanov and V.Y. Aresenin, Solutions of ill-posed problems (Wiley, New York, 1977).
[2] FERDOR AND COOLC, RSIC code package PSR-17, Radiation Shielding Information Center, Oak Ridge National Laboratory.
[3] M.J. Coolbaugh, R.E. Faw and W. Meyer, Kansas State University, USAEC Document No. COO-2049-7 (1971).
[4] E.F. Bennett and T.J. Yule, Argonne National Laboratory, ANL-7763 (1971).
[5] W.H. Miller, Nucl. Instr. and Meth. 153 (1978) 535.
[6] R.H. Johnson, Proc. Radiation Shielding Information Center Seminar-Workshop, ORNL-RSIC 40 (1976).
[7] J. Bok, Comp. Phys. Comm. 16 (1978) 113.
[8] V.V. Verbinski, W.R. Burrus, T.A. Lone, W. Zobel and N.W. Hill, Nucl. Instr. and Meth. G5 (1968) 8.
[9] K.W. Geiser, Proc. IAEA Consultants' Meeting on Neutron source properties, Debrecen, Hungary, INDC(NDS)-114/GT, (1980) p. 43.
[10] Use of rare earth oxides in concrete for reactor shields, Final Report on the IAEA Research Contract 2253/R1/RB (1983).